Effect of Kurtosis-type of Primordial Non-Gaussianity on Halo Mass Function

arXiv:1103.2586

Nagoya University/IPMU, U. Tokyo

Naoshi Sugiyama

with **Shuichiro Yokoyama**, Joe Silk, Saleem Zaroubi

Utilize (1)void abundance (2)early star formation (3)most massive object at high z, as a probe of "non-skewed" non-Gaussianity

Kurtosis type non-Gaussianity

- Kurtosis: 4th order, non-Skewed

$$\zeta = \zeta_G + \frac{3}{5} f_{NL} \left(\zeta_G^2 - \langle \zeta_G^2 \rangle \right) + \frac{9}{25} \boxed{g_{NL}} \zeta_G^3$$

Trispectrum can be written as:

$$\langle \zeta(\mathbf{k}_1)\zeta(\mathbf{k}_2)\zeta(\mathbf{k}_3)\zeta(\mathbf{k}_4) \rangle = (2\pi)^3 T_\zeta(k_1,k_2,k_3,k_4)\delta^{(3)}\left(\mathbf{k}_1+\mathbf{k}_2+\mathbf{k}_3+\mathbf{k}_4\right) \ ,$$

$$T_\zeta(k_1,k_2,k_3,k_4) = \boxed{\tau_{NL}} \left(P_\zeta(k_1)P_\zeta(k_2)P_\zeta(k_{13}) + 11\text{perms.} \right) + \frac{54}{25} g_{NL} \left(P_\zeta(k_1)P_\zeta(k_2)P_\zeta(k_3) + 3\text{perms.} \right)$$

$$\tau_{NL} = \frac{36}{25} f_{NL}^2$$

This is true, only when primordial fluctuations are generated from a single scalar field.

For multi-field inflation, τ_{NL} is a parameter but with constraint:

$$\tau_{NL} \geqslant \frac{36}{25} f_{NL}^2$$

Unlike g_{NL} τ_{NL} has a lower bound.
Set a constraint on multi-field inflation.

T. Suyama and M. Yamaguchi 2008

Kurtosis type non-Gaussianity

- Kurtosis: 4th order, non-Skewed

$$\zeta = \zeta_{\rm G} + \frac{3}{5} f_{\rm NL} \left(\zeta_{\rm G}^2 - \langle \zeta_{\rm G}^2 \rangle \right) + \frac{9}{25} \boxed{g_{\rm NL}} \zeta_{\rm G}^3$$

Trispectrum can be written as:

$$\langle \zeta(\mathbf{k}_1)\zeta(\mathbf{k}_2)\zeta(\mathbf{k}_3)\zeta(\mathbf{k}_4) \rangle = (2\pi)^3 T_\zeta(k_1, k_2, k_3, k_4) \delta^{(3)} \left(\mathbf{k}_1 + \mathbf{k}_2 + \mathbf{k}_3 + \mathbf{k}_4 \right) ,$$

$$T_\zeta(k_1, k_2, k_3, k_4) = \boxed{\tau_{\rm NL}} \left(P_\zeta(k_1) P_\zeta(k_2) P_\zeta(k_{13}) + 11 \text{perms.} \right) + \frac{54}{25} g_{\rm NL} \left(P_\zeta(k_1) P_\zeta(k_2) P_\zeta(k_3) + 3 \text{perms.} \right)$$

$$\tau_{\rm NL} = \frac{36}{25} f_{\rm NL}^2$$

This is true, only when primordial fluctuations are generated from a single scalar field.

For multi-field inflation, $\tau_{\rm NL}$ is a parameter but with constraint:

$$\tau_{\rm NL} \geq \frac{36}{25} f_{\rm NL}^2 \ /2$$

Eiichiro's Talk

T. Suyama and M. Yamaguchi 2008

Probability Distribution Func.

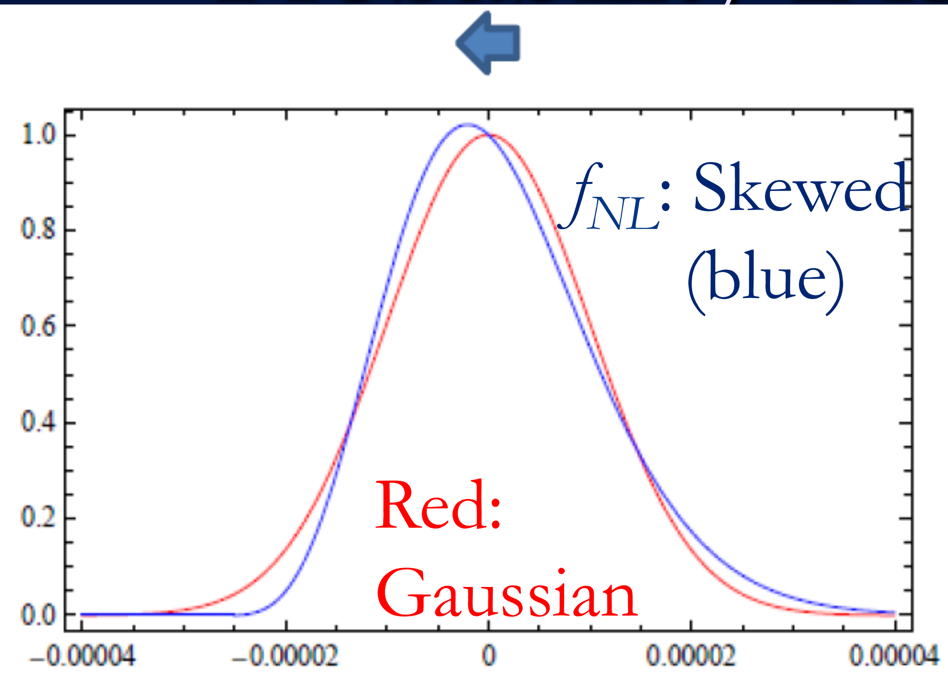

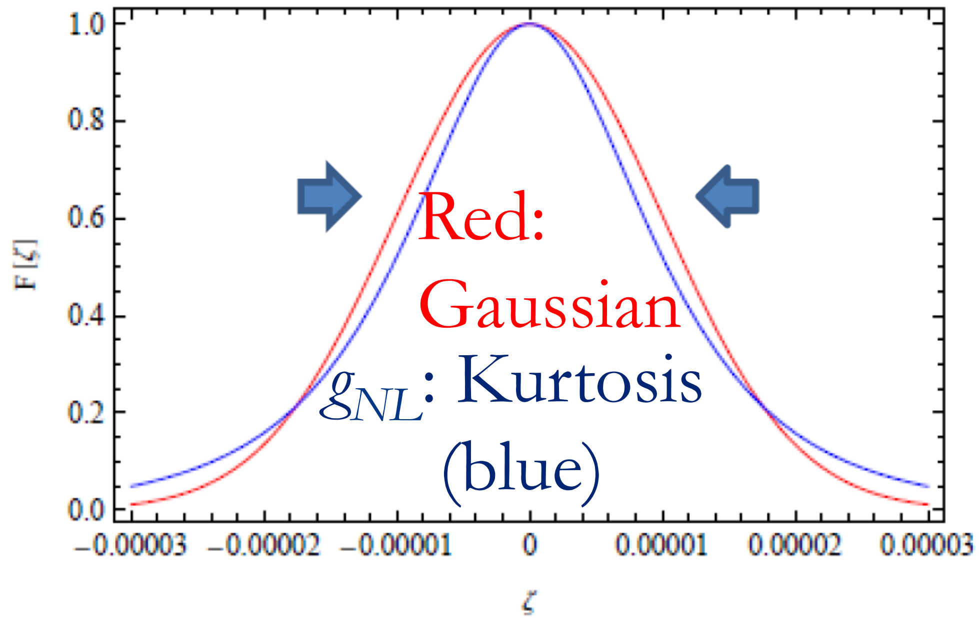

Probability Distribution Func.

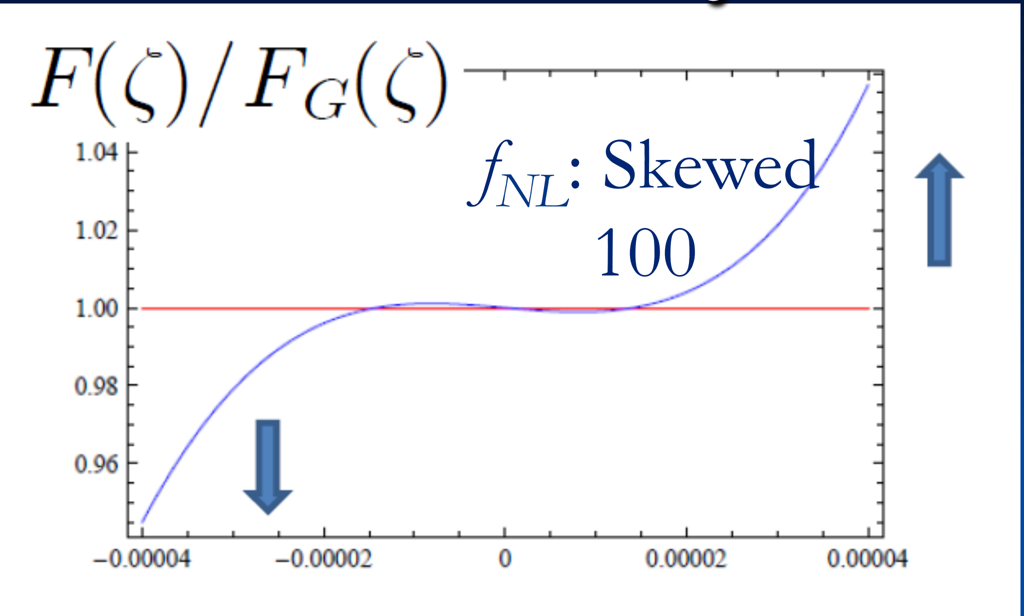

Take the ratio
with Gaussian case

Huge Difference in the tails
Distinguishable?

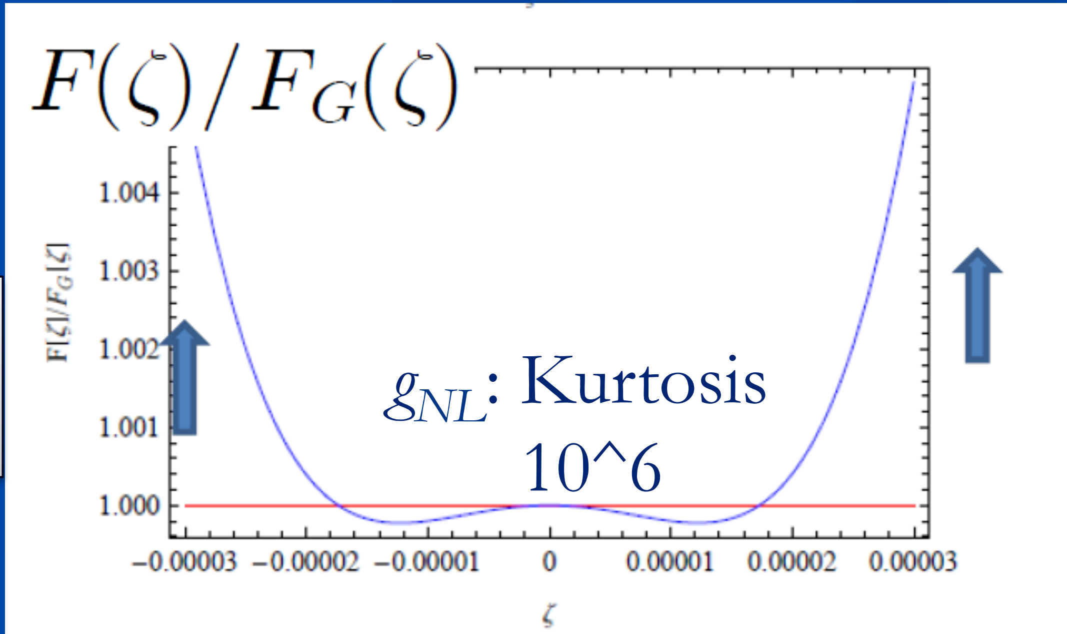

Limits from WMAP

- $-10 < f_{\rm NL} < 74$ (95%CL)
- $-7.4\times10^5 < g_{\rm NL} < 8.2\times10^5$
- $-0.6\times10^4 < \tau_{\rm NL} < 3.3\times10^4$

Komatsu et al. 2010

Smidt, Amblard, Byrnes, Cooray, Heavens, Munshi 2010

Here, in order to see the effect in the clear manner, we take $\tau_{\rm NL} = 10^6$

Non-Gaussian Mass Function

- Mass Function: Number of Collapsed Objects

Probability Density Function (PDF) is needed

$$\delta_R = \int \frac{d^3\mathbf{k}}{(2\pi)^3} W_R(k)\delta(\mathbf{k}, z)$$

$$W_R(k) = 3\left(\frac{\sin(kR)}{k^3R^3} - \frac{\cos(kR)}{k^2R^2}\right)$$

$F(\delta_R)d\delta_R$: PDF of δ_R

$$\langle \delta_R^n \rangle \equiv \int_{-\infty}^{\infty} \delta_R^n F(\delta_R) d\delta_R$$

n-th central moment

$$S_p(R) \equiv \frac{\langle \delta_R^p \rangle_c}{\langle \delta_R^2 \rangle_c^{p-1}}$$

p-th reduced cumulant

S_3: skewness
S_4 : kurtosis

$$\langle \delta_R \rangle_c = 0\ ,\ \langle \delta_R^2 \rangle_c = \langle \delta_R^2 \rangle \equiv \sigma_R^2\ ,$$

$$\langle \delta_R^3 \rangle_c = \langle \delta_R^3 \rangle\ ,\ \langle \delta_R^4 \rangle_c = \langle \delta_R^4 \rangle - 3\langle \delta_R^2 \rangle_c^2$$

Probability Distribution Func.

- Edgeworth expansion   Juszkiewicz et al.95, LoVerde et al.08

$$F(\nu)d\nu = d\nu\left[c_0F_G(\nu) + \sum_{m=1}\frac{c_m}{m!}(-1)^m H_m(\nu)F_G(\nu)\right]$$

$$F_G(\nu) \equiv (2\pi)^{-1/2}\exp(-\nu^2/2)$$

Coefficients can be evaluated:

$$c_0 = 1\,,\; c_1 = c_2 = 0\,,\; c_3 = -S_3(R)\sigma_R\,,\; c_4 = S_4(R)\sigma_R^2\,,$$
$$c_5 = -S_5(R)\sigma_R^3\,, c_6 = 10S_3(R)^2\sigma_R^2 + S_6(R)\sigma_R^4\,,\cdots\,,$$

Non-Gaussian PDF can be obtained:

$$F(\nu)d\nu = \frac{d\nu}{\sqrt{2\pi}}\exp\left(-\nu^2/2\right)\left[1 + \frac{S_3(R)\sigma_R}{6}H_3(\nu) + \frac{1}{2}\left(\frac{S_3(R)\sigma_R}{6}\right)^2 H_6(\nu) + \frac{1}{6}\left(\frac{S_3(R)\sigma_R}{6}\right)^3 H_9(\nu)\right.$$
$$\left. + \frac{S_4(R)\sigma_R^2}{24}H_4(\nu) + \frac{1}{2}\left(\frac{S_4(R)\sigma_R^2}{24}\right)^2 H_8(\nu) + \frac{1}{6}\left(\frac{S_4(R)\sigma_R^2}{24}\right)^3 H_{12}(\nu) + \cdots\right],$$

D'Amico et al. 2010

Halo Mass Function

$$
\begin{aligned}
\frac{dn}{dM}(M,z)dM &= -dM\frac{2\bar\rho}{M}\frac{d}{dM}\int_{\delta_c/\sigma_R}^{\infty} d\nu F(\nu) \\
&= -dM\sqrt{\frac{2}{\pi}}\frac{\bar\rho}{M}\exp\left[-\frac{\nu_c^2}{2}\right]\left\{\frac{d\ln\sigma_R}{dM}\nu_c\left[1\right.\right. \\
&\quad +\frac{S_3(R)\sigma_R}{6}H_3(\nu_c)+\frac{1}{2}\left(\frac{S_3(R)\sigma_R}{6}\right)^2 H_6(\nu_c)+\frac{1}{6}\left(\frac{S_3(R)\sigma_R}{6}\right)^3 H_9(\nu_c) \\
&\quad \left.+\frac{S_4(R)\sigma_R^2}{24}H_4(\nu_c)+\frac{1}{2}\left(\frac{S_4(R)\sigma_R^2}{24}\right)^2 H_8(\nu_c)+\frac{1}{6}\left(\frac{S_4(R)\sigma_R^2}{24}\right)^3 H_{12}(\nu_c)\right] \\
&\quad +\frac{d}{dM}\left(\frac{S_3(R)\sigma_R}{6}\right)H_2(\nu_c)+\frac{1}{2}\frac{d}{dM}\left(\frac{S_3(R)\sigma_R}{6}\right)^2 H_5(\nu_c)+\frac{1}{6}\frac{d}{dM}\left(\frac{S_3(R)\sigma_R}{6}\right)^3 H_8(\nu_c) \\
&\quad \left.+\frac{d}{dM}\left(\frac{S_4(R)\sigma_R^2}{24}\right)H_3(\nu_c)+\frac{1}{2}\frac{d}{dM}\left(\frac{S_4(R)\sigma_R^2}{24}\right)^2 H_7(\nu_c)+\frac{1}{6}\frac{d}{dM}\left(\frac{S_4(R)\sigma_R^2}{24}\right)^3 H_{11}(\nu_c)\right\}+
\end{aligned}
$$

NG term

Ratio to Gaussian Mass Function

$$\mathrm{R_{NG}}(M,z)\equiv\frac{dn(M,z)/dM}{dn_{\mathrm{G}}(M,z)/dM}$$

$$\frac{dn_{\mathrm{G}}}{dM}(M,z)dM=-\sqrt{\frac{2}{\pi}}\frac{\bar\rho}{M}\exp\left[-\frac{\nu_c^2}{2}\right]\frac{d\ln\sigma_R}{dM}\nu_c dM$$

Fitting: Skewness & Kurtosis

In the squeezed limit (local type)

- Skewness

$$\sigma_R S_3(R) = 4.3 \times 10^{-4} f_{\rm NL} \times \sigma_R^{0.13} \;\; (10^{12} h^{-1} M_\odot < M < 2 \times 10^{15} h^{-1} M_\odot)$$

De Simone, Maggiore & Riotto 2010; Enqvist, Hotchkiss & Taanila 2010

- Kurtosis

from $g_{\rm NL}$

$$\sigma_R^2 S_4^g(R) \quad = \quad 9.4 \times 10^{-8} g_{\rm NL} \times \sigma_R^{0.27} \;\; (10^{12} h^{-1} M_\odot < M < 2 \times 10^{15} h^{-1} M_\odot)$$

Chongchitnan & Silk 2010a; Enqvist, Hotchkiss & Taanila 2010

from $\tau_{\rm NL}$

$$\sigma_R^2 S_4^\tau(R) \quad = \quad 1.9 \times 10^{-7} \tau_{\rm NL} \times \sigma_R^{0.25} \;\; (10^{12} h^{-1} M_\odot < M < 2 \times 10^{15} h^{-1} M_\odot)$$

Mass Function

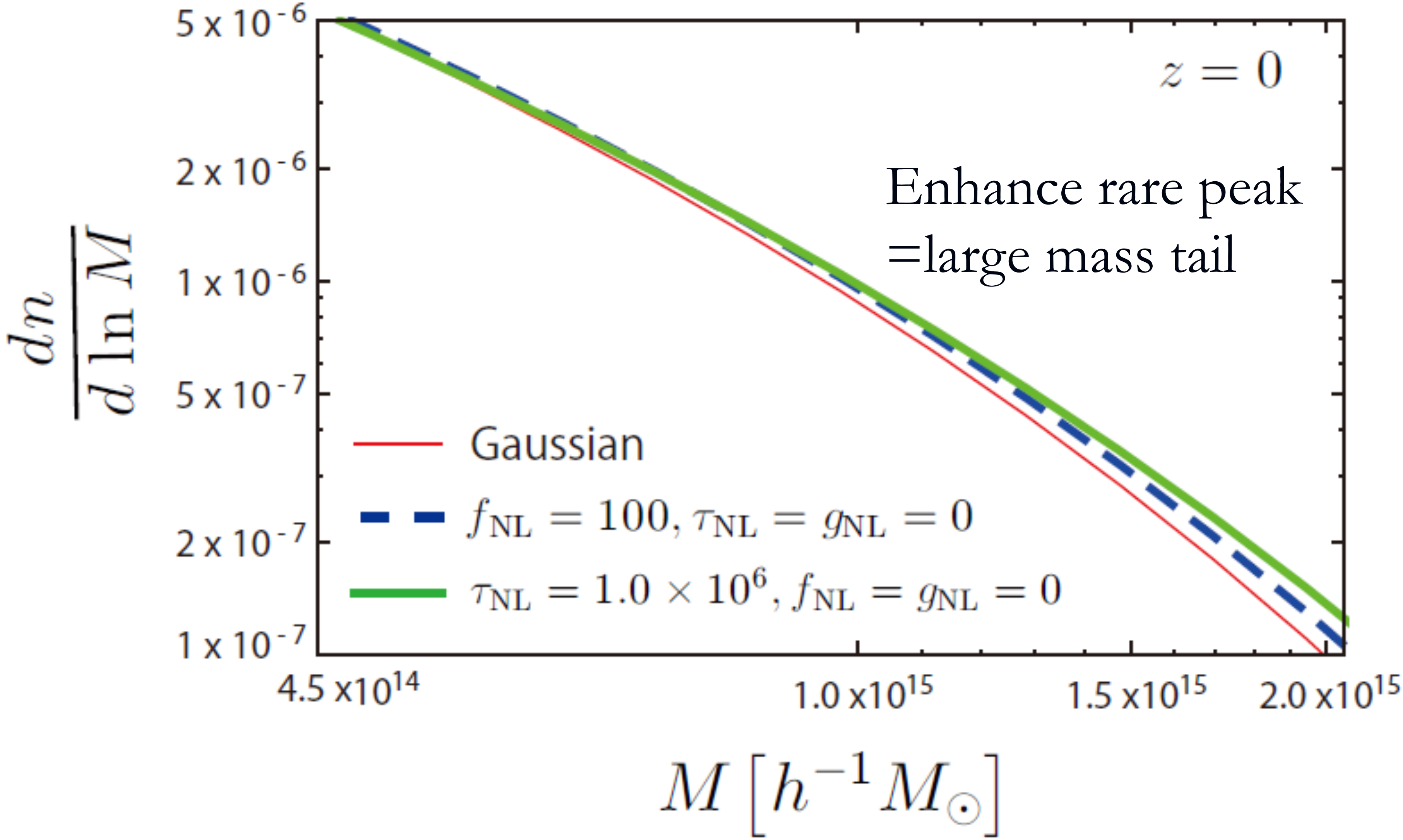

Mass Function (ratio to Gauss)

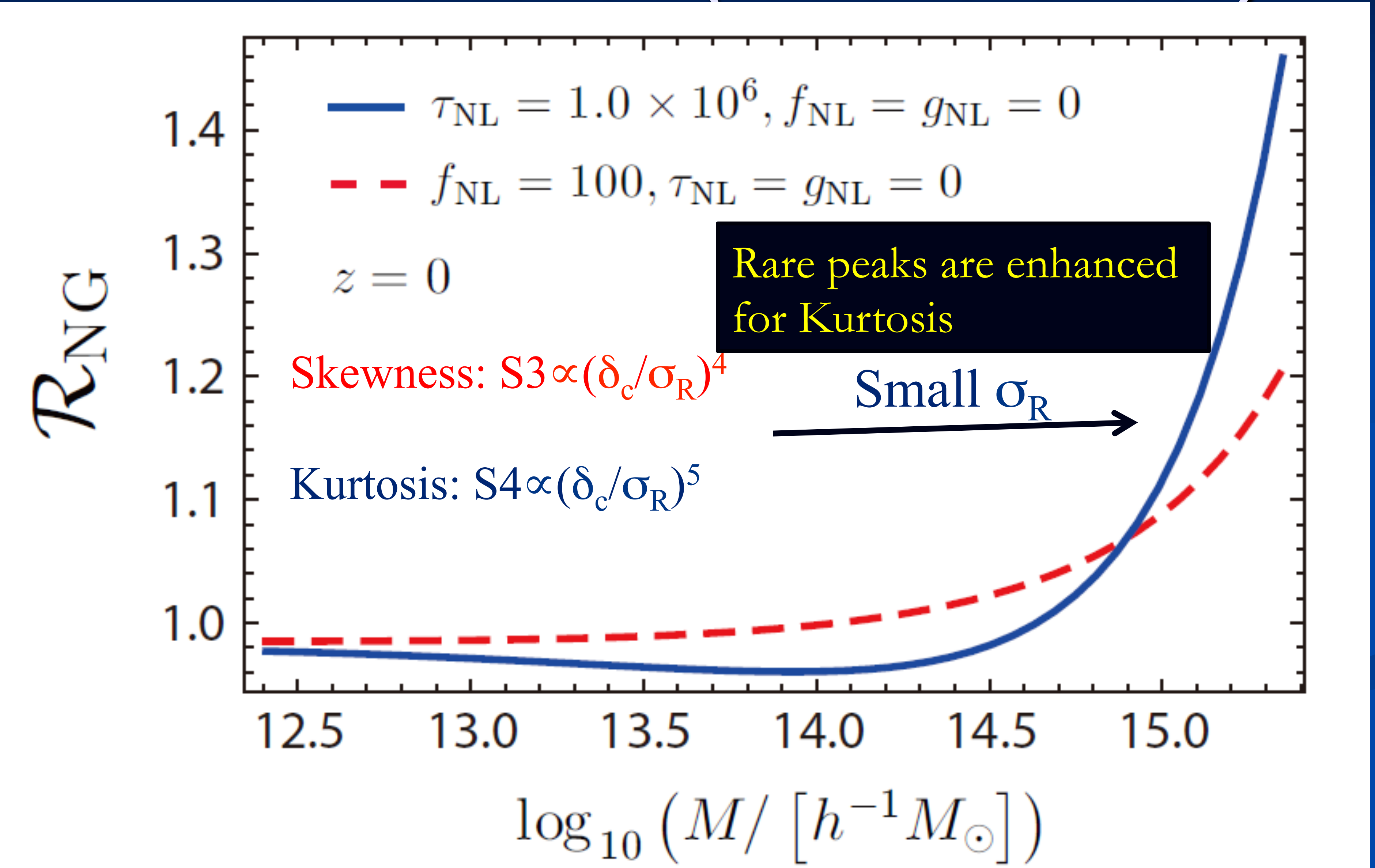

Application 1: Early Star Formation

- A simple analytic model

Somerville, et al. 2003

global star formation density

$$\dot{\rho}_* = e_* \rho_b \frac{d}{dt} F_h(M_{\rm vir} > M > M_{\rm crit}, t)$$

e_*: star formation efficiency: 0.001 – 0.002
M_{crit}: minimum collapsed mass: $10^6 h^{-1} M_{SUN}$
M_{vir}: virial mass $T_{vir}=10^4$K
F_h: fraction of the total mass in collapsed objects

$$F_h(M_{\rm vir} > M > M_{\rm crit}, z) = \frac{1}{\bar{\rho}} \int_{M_{\rm crit}}^{M_{\rm vir}} M \frac{dn}{dM}(M, z) dM$$

⇦ NG

⇩

$$\frac{dn_\gamma}{dt}(t) = e_* \rho_b N_\gamma \left(F_h(t) - F_h(t - \tau_{\rm III}) \right)$$

N_γ: # of photons/s/M_{SUN}
τ_{III}: life time of PopIII star

Application 1: Early Star Formation

Cumulative # of ionizing photons/baryons

$$\frac{n_\gamma}{n_H}(z) \simeq \mu m_p e_* N_\gamma F_h(M_{\rm vir} > M > M_{\rm crit}, z)\tau_{\rm III}$$

Good measure of reionization of inter galactic medium

Apprrox. $n_\gamma/n_H = 10$ is the epoch of reionization

Time evolution of Cumulative number of ionizing photons

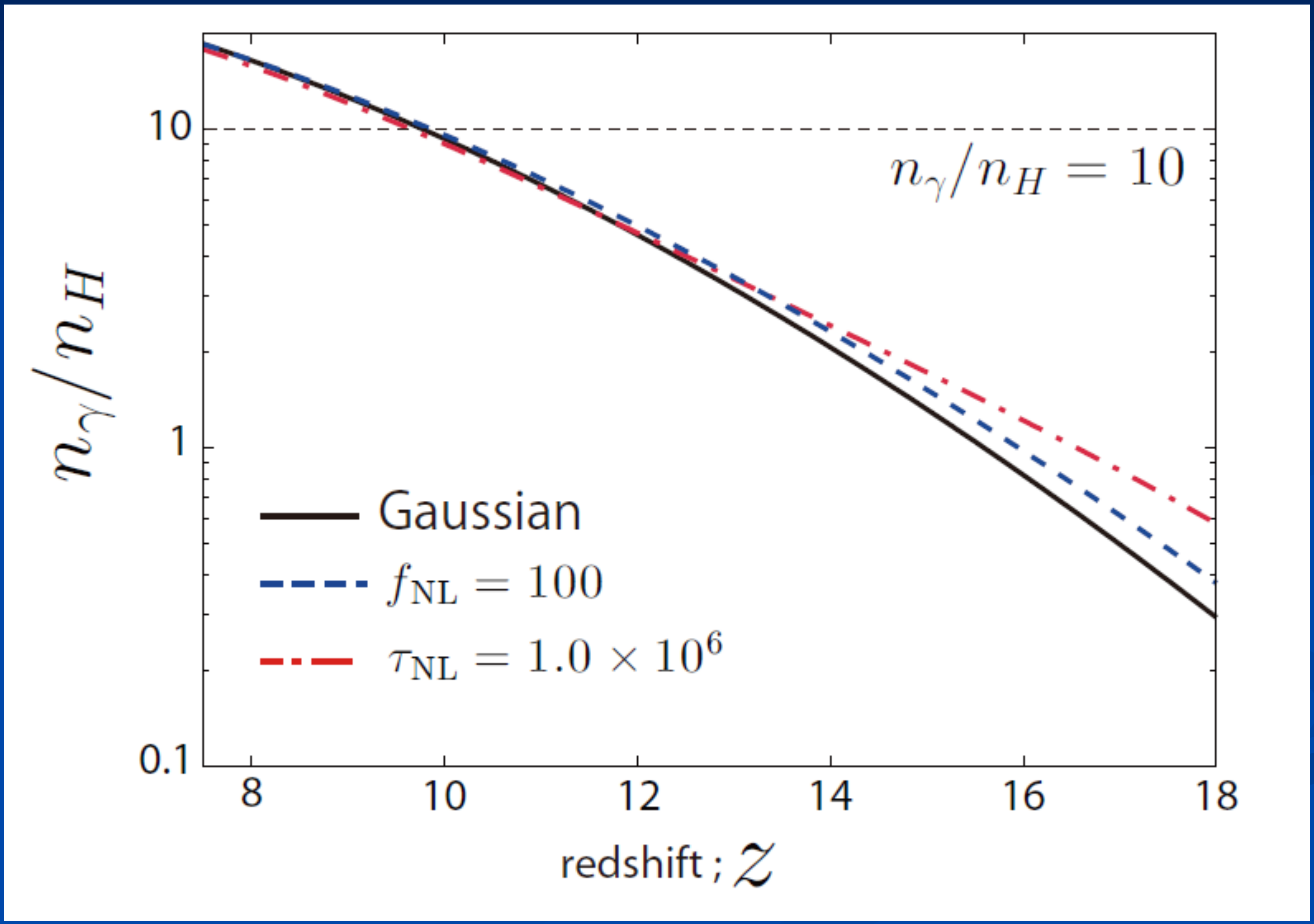

Time evolution of Cumulative number of ionizing photons
Non-Gaussian vs Gaussian

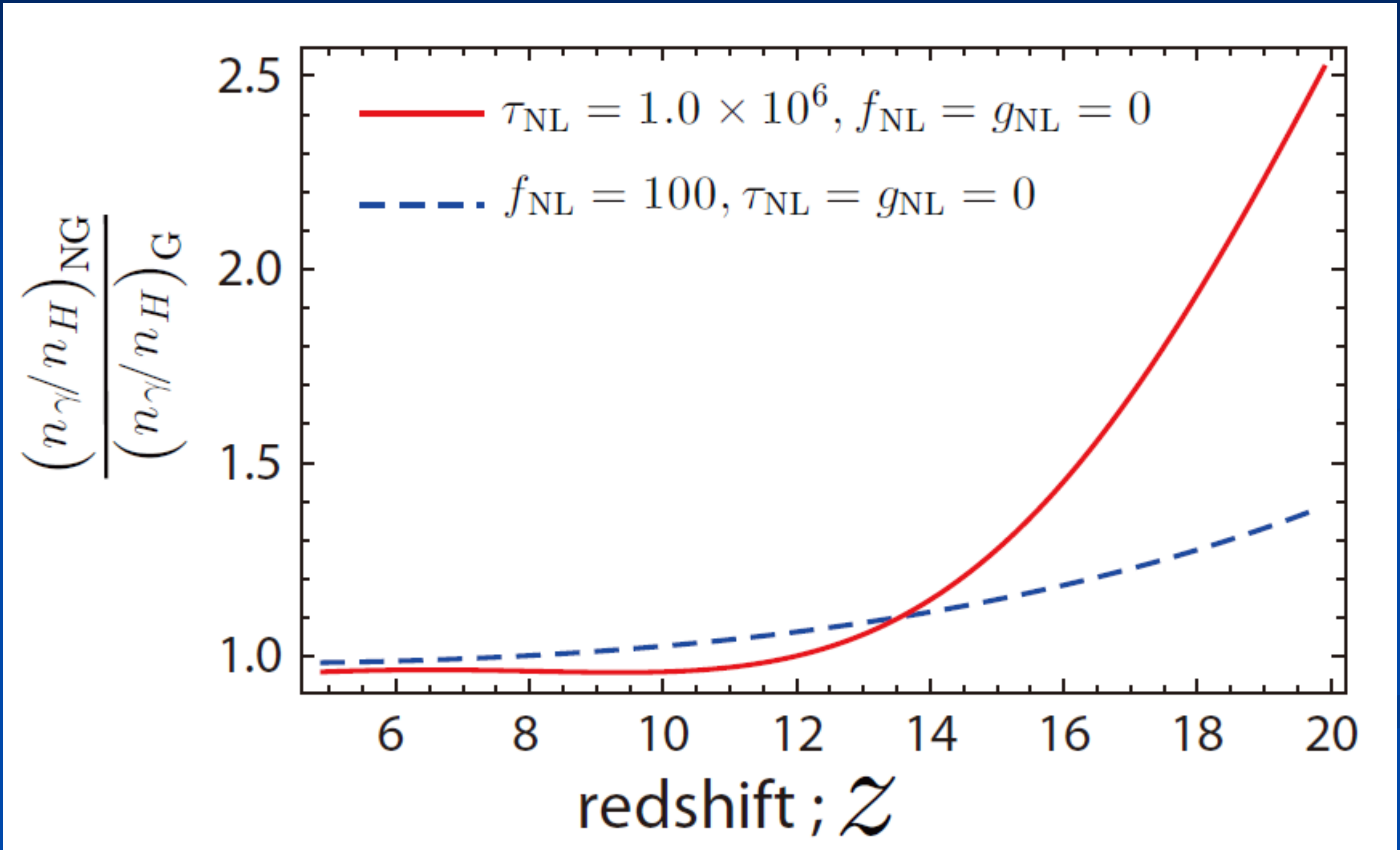

Application 1: Early Star Formation

- Non-Gaussianity doesn’t affect much about global reionization history
- For the first star formation, however, non-Gaussisan, especially Kurtosis type one enhances reionization a lot!

Application 2. High-Redshift Massive Clusters

- XMMU J2235.3-2557

  at $z=1.4$, $M=(6.4\pm1.2)\times10^{14}M_{SUN}$

  - Cayon et al. found to explain this, $\boxed{f_{NL}=449}$ is needed

Ruled out by WMAP constraints

⇩

This f_{NL} corresponds to $\tau_{NL}=1.7\times10^{6}$
to obtain same R_{NG}

Application 3. Void Abundance

Press Schechter

Kamionkowski, Verde, Jimenez 2009

$$\frac{dn^{\rm void}(R)}{dR}dR = -dR \times \frac{6}{4\pi R^3}\frac{d}{dR}\int_{-\infty}^{\delta_v/\sigma_R} F(\nu)d\nu$$

- Gaussian

$$\frac{dn_G^{\rm void}(R)}{dR} = \sqrt{\frac{2}{\pi}}\frac{3}{4\pi R^4}\exp\left[-\frac{\delta_v^2}{2\sigma_R^2}\right]\frac{\delta_v}{\sigma_R}\frac{d\ln\sigma_R}{d\ln R}$$

- Non-Gaussian

$$\begin{aligned}\frac{dn^{\rm void}(R)}{dR} \;=\; & \sqrt{\frac{2}{\pi}}\frac{3}{4\pi R^4}\exp\left[-\frac{\delta_v^2}{2\sigma_R^2}\right]\left\{\frac{d\ln\sigma_R}{d\ln R}\frac{\delta_v}{\sigma_R}\left[1\right.\right.\\ & \left.+\frac{S_3(R)\sigma_R}{6}H_3(\delta_v/\sigma_R)+\frac{S_4(R)\sigma_R^2}{24}H_4(\delta_v/\sigma_R)\right]\\ & \left.+\frac{d}{d\ln R}\left(\frac{S_3(R)\sigma_R}{6}\right)H_2(\delta_v/\sigma_R)+\frac{d}{d\ln R}\left(\frac{S_4(R)\sigma_R^2}{24}\right)H_3(\delta_v/\sigma_R)\right]\end{aligned}$$

Void Abundance as a function of the size of void, R

Ratio between non-Gaussian and Gaussian cases

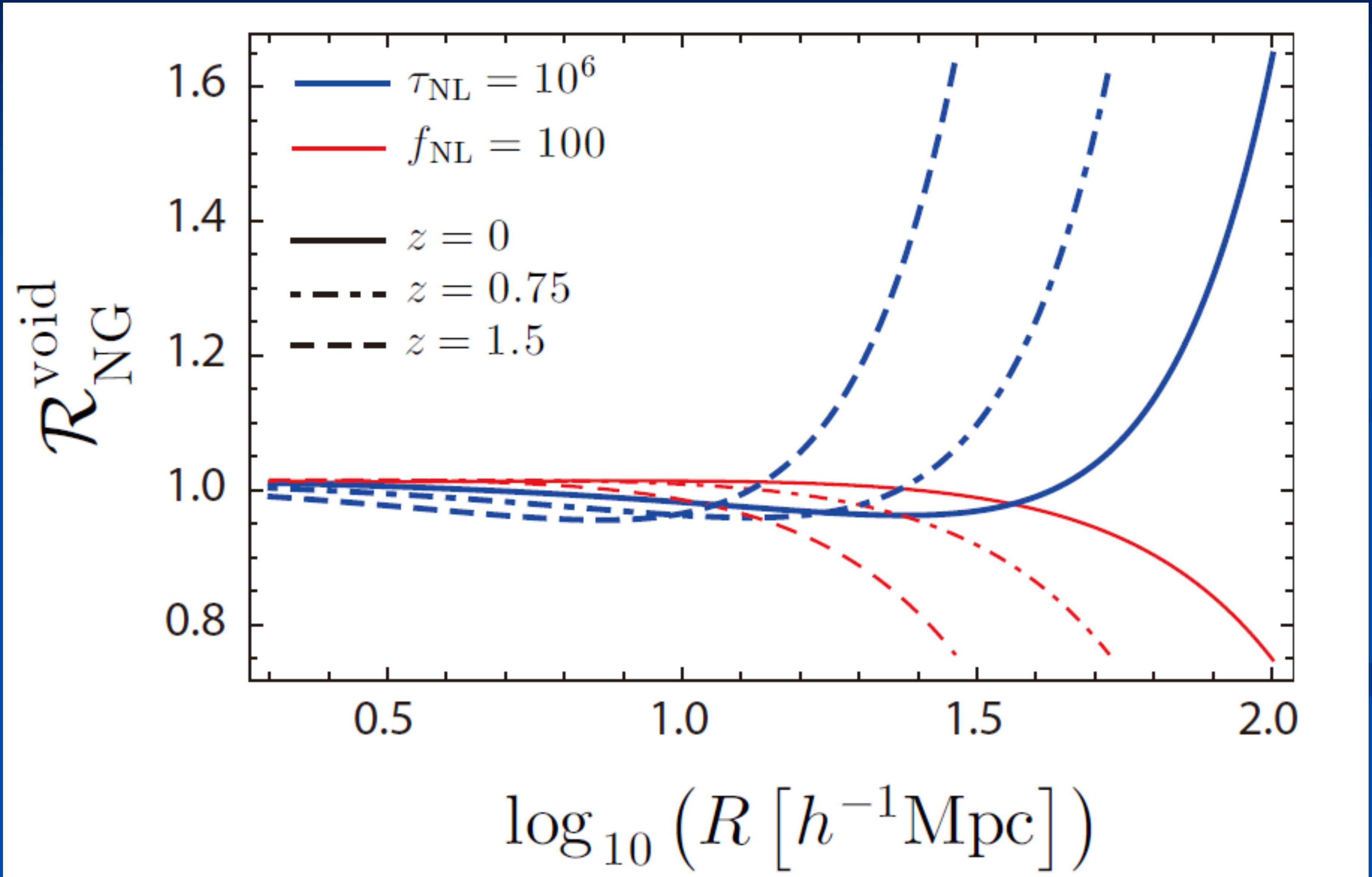

Application 3. Void Abundance

- Since it reflects the negative tail of the distribution function, τ_{NL} and f_{NL} work opposite directions
  - Positive τ_{NL} increases void abundance
  - Positive f_{NL} decreases void abundance

Combining Void abundance with other observations, e.g., massive cluster, early star formation, we can make a distinction between skewed and non-skewed non-Gaussian distribution

Summary

- We study the effect of the Kurtosis type primordial non-Gaussianity on structure formation.
  - obtain a formula of the halo mass function with primordial non-Gaussianities, including f_{NL}, g_{NL}, τ_{NL}
  - find the enhancement of the formation of the massive and high redshift objects, especially high density peak object for the Kurtosis type.
    - early phase of reionization of the Universe
    - massive clusters at high redshift
    - abundance of voids
- potential to distinguish skewness & kurtosis types

Another application of the mass function

Ionized bubble number count as a probe of non-Gaussianity

Hiroyuki Tashiro[1], and Naoshi Sugiyama[2,3,4]

[1] *Center for Particle Physics and Phenomenology (CP3), Université catholique de Louvain, Chemin du Cyclotron, 2, B-1348 Louvain-la-Neuve, Belgium*

[2] *Department of Physics and Astrophysics, Nagoya University, Chikusa, Nagoya 464-8602, Japan*

[3] *Institute for Physics and Mathematics of the Universe, University of Tokyo, 5-1-5 Kashiwa-no-Ha, Kashiwa, Chiba, 277-8582, Japan*

[4] *Kobayashi-Maskawa Institute for the Origin of Particles and the Universe, Nagoya University,*

arXiv:1104.0139

- Utilize the number of Ionized bubbles at the epoch of reionization as a probe of non-Gaussianity

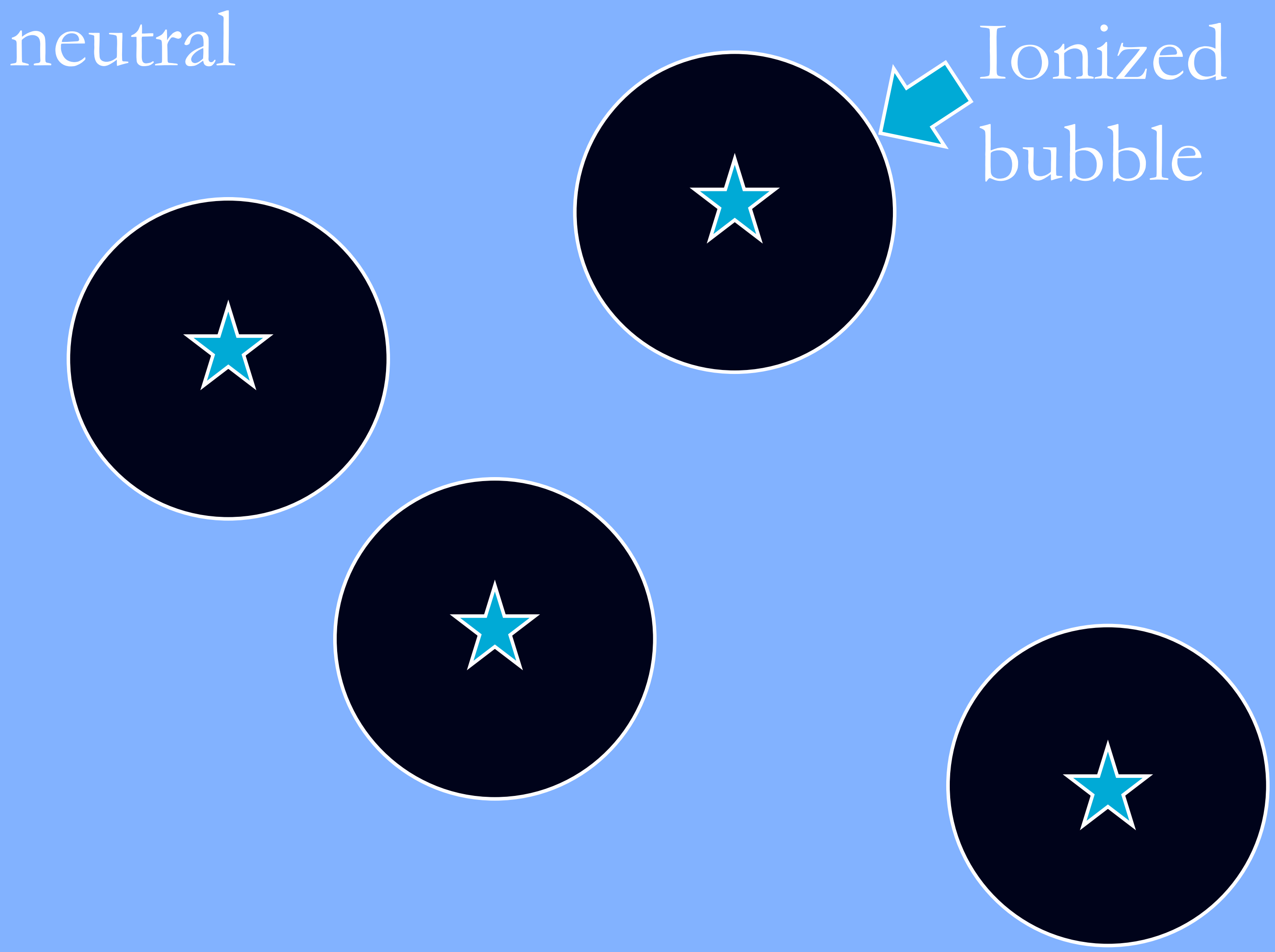
neutral
Ionized
bubble

Simple Analytic Model of Ionized Bubbles

- Dark Halo whose virial temperature >10^4K collapses, and forms spherical halo
- Size of ionized bubble (Loeb et al. 2005)

$$R_{\rm max} = 0.138\, f_{\rm esc}^{1/3} \left(\frac{M}{10^9\, M_\odot}\right)^{1/3} \left(\frac{1+z}{11}\right)^{-1} \times \left(\frac{\Omega_m h^2}{0.14}\right)^{-1/3} \left(\frac{N_\gamma f_*}{430}\right)^{1/3} \text{Mpc}$$

  - fesc : escape fraction of photons, assumed to be 0.05
  - N γ : number of ionized photons per baryon in stars, 43,000 (Bromm et al . 2001)
  - f_*: star formation efficiency, 0.05

Number Count of Ionized Bubbles

- Bubbles are detected as holes in 21cm map
- In actual observations, holes are smeared…

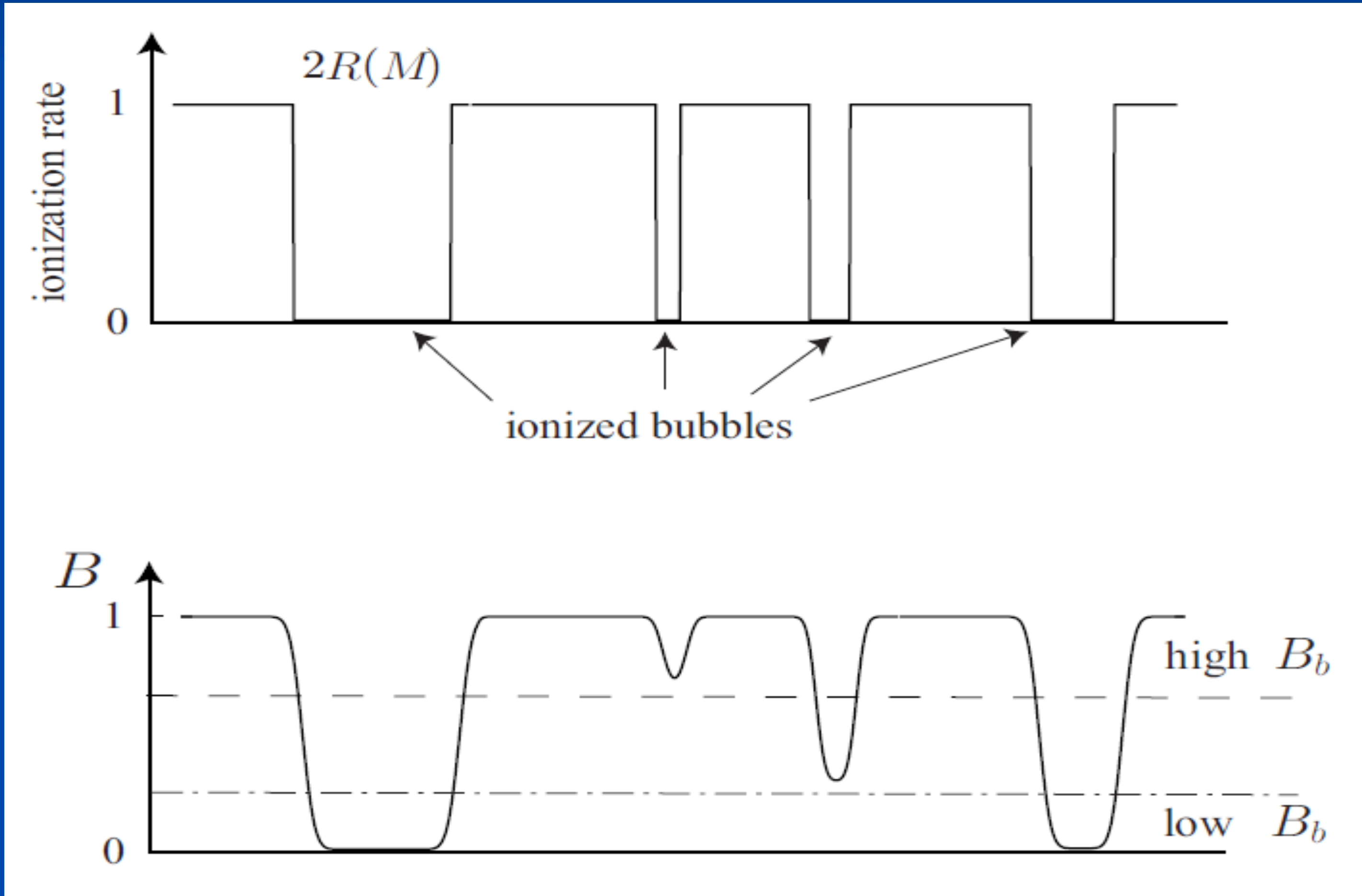

- Surface brightness temperature contrast of an ionized bubble (hole or not hole)

$$B(\theta, z) = \frac{Y_{obs}(\theta, z)}{T_{21}(z) \int d\Omega' \ \exp\left[-\frac{\theta'^2}{2\sigma^2}\right]}$$

  - $\sigma = \theta_{\rm FWHM}/\sqrt{8\ln 2}$ Gaussian resolution
  - $T_{21}(z)$: 21cm background temperature
  - $Y_{obs}(\theta)$: surface brightness temperature

$$Y_{obs}(\theta, z) = \int d\Omega' \ T(\theta - \theta', z) \exp\left[-\frac{(\theta - \theta')^2}{2\sigma^2}\right]$$

  - Angular profile $T(\theta,z)$

$$T(\theta, z) = \begin{cases} 0, & \theta < \theta_R \\ T_{21}(z), & \theta > \theta_R \end{cases}$$

Criterion of bubble detection

- Parameter B_b: assume bubbles with B smaller than B_b can be detected

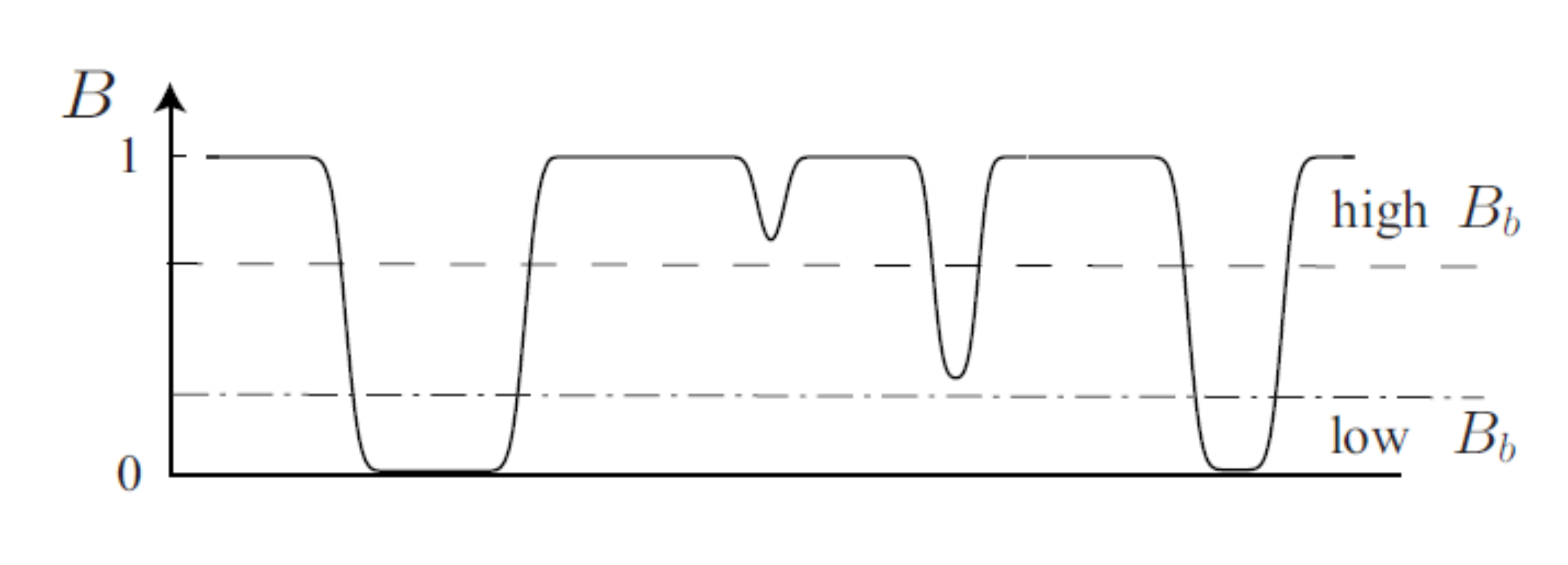

- Number count of detectable bubbles

$$N(< B_b) = \int_{M_{\mathrm{lim}}(B_b)} dM \frac{dV}{dz} \frac{dn}{dM} \Delta z$$

Possible observations

- Angular resolution $\theta_{FWHM}=\lambda/D$
  - λ: frequency, $=21(1+z)$cm
  - D: baseline length

    low resolution(LOFAR) 2km

    high resolution(SKA) 5km

Density dispersion & Skewness

- Non-Gaussianity

$$\Phi(\boldsymbol{x}) = \Phi_{\rm G}(\boldsymbol{x}) + f_{NL}(\Phi_{\rm G}^2(\boldsymbol{x}) - \langle \Phi_{\rm G}^2(\boldsymbol{x}) \rangle)$$

- Power spectrum P(k)

$$\langle \Phi_{\rm G}(\boldsymbol{k}) \Phi_{\rm G}(\boldsymbol{k}') \rangle = (2\pi)^3 \delta_D(\boldsymbol{k} + \boldsymbol{k}') P(k)$$

- Smoothed density dispersion

$$\sigma_M^2(M) = \langle \delta_R^2 \rangle = \int \frac{dk^3}{(2\pi)^3} W(R,k)^2 D(k,z)^2 P(k).$$

- Smoothed Skewness

$$S_3(M) \equiv \frac{\langle \delta_R^3 \rangle}{\langle \delta_R^2 \rangle^2}$$

- Here:

$$\langle \delta_R^3 \rangle = \int \frac{d^3k_1}{(2\pi)^3} \frac{d^3k_2}{(2\pi)^3} \frac{d^3k_3}{(2\pi)^3} W(R,k_1) W(R,k_2) W(R,k_3) \times D(k_1,z) D(k_2,z) D(k_3,z) \langle \Phi(k_1) \Phi(k_2) \Phi(k_3) \rangle$$

Mass Function

- Mass Function

$$\frac{dn(M,z)}{dM} = -\sqrt{\frac{2}{\pi}}\frac{\bar{\rho}}{M}\exp\left[-\frac{\delta_c^2}{2\sigma_M^2}\right]\mathcal{R}_{NG}$$

  - Here:

$$\mathcal{R}_{NG} = \left[\frac{d\ln\sigma_M}{dM}\left(\frac{\delta_c}{\sigma_M}+\frac{S_3\sigma_M}{6}\left(\frac{\delta_c^4}{\sigma_M^4}-2\frac{\delta_c^2}{\sigma_M^2}-1\right)\right)\right.$$
$$\left.+\frac{1}{6}\frac{dS_3}{dM}\sigma_M\left(\frac{\delta_c^2}{\sigma_M^2}-1\right)\right],$$

Non-Gaussian comes through S_3 terms

f_{NL} dependence of $N(<B_b)$

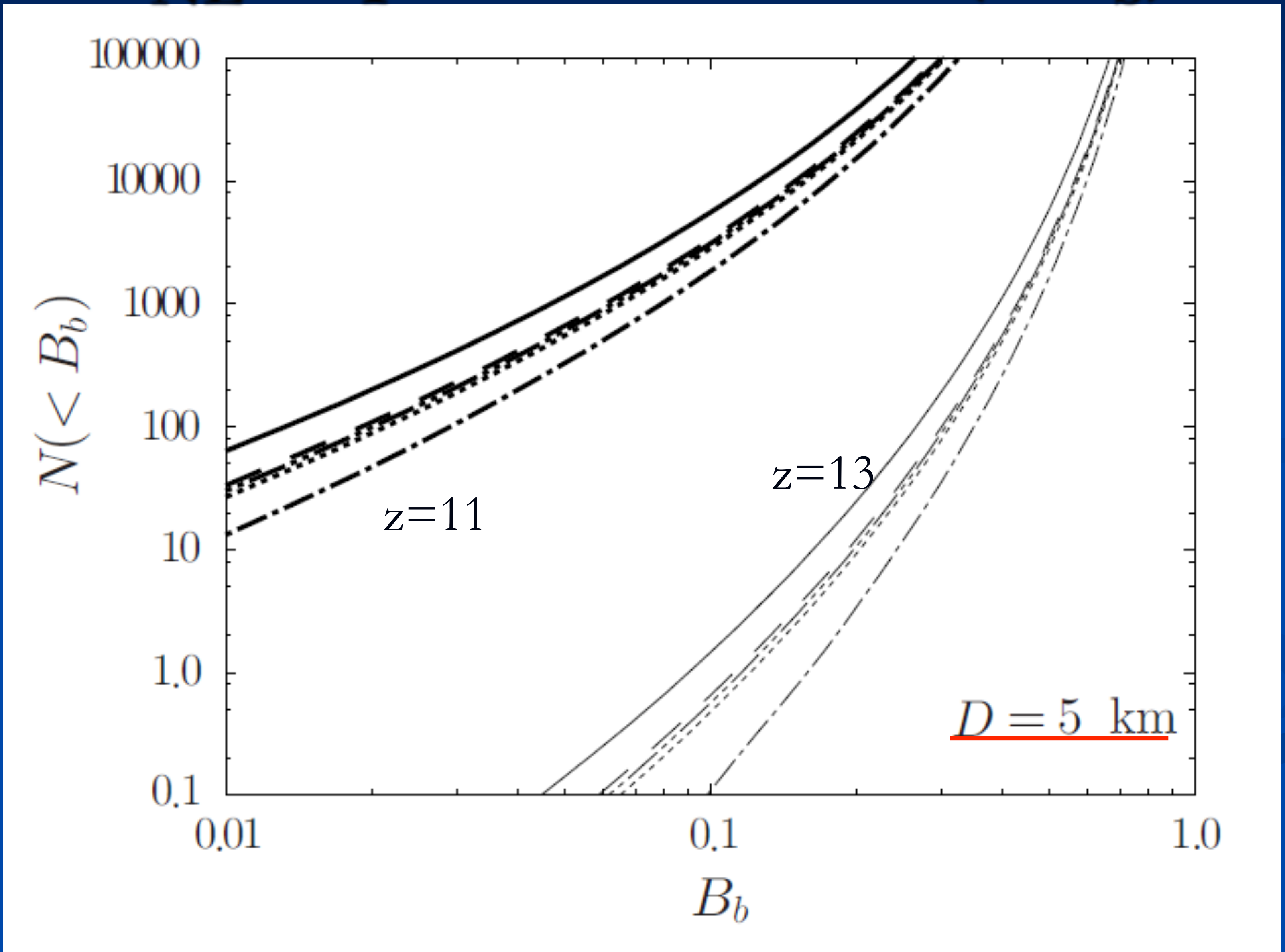

f_{NL} dependence of $N(<B_b)$

- Large positive f_{NL} produces more number of bubbles from non-Gaussian tail
- At higher z
  - less number of bubbles produced for same B_b
  - smaller bubbles (large B_b)

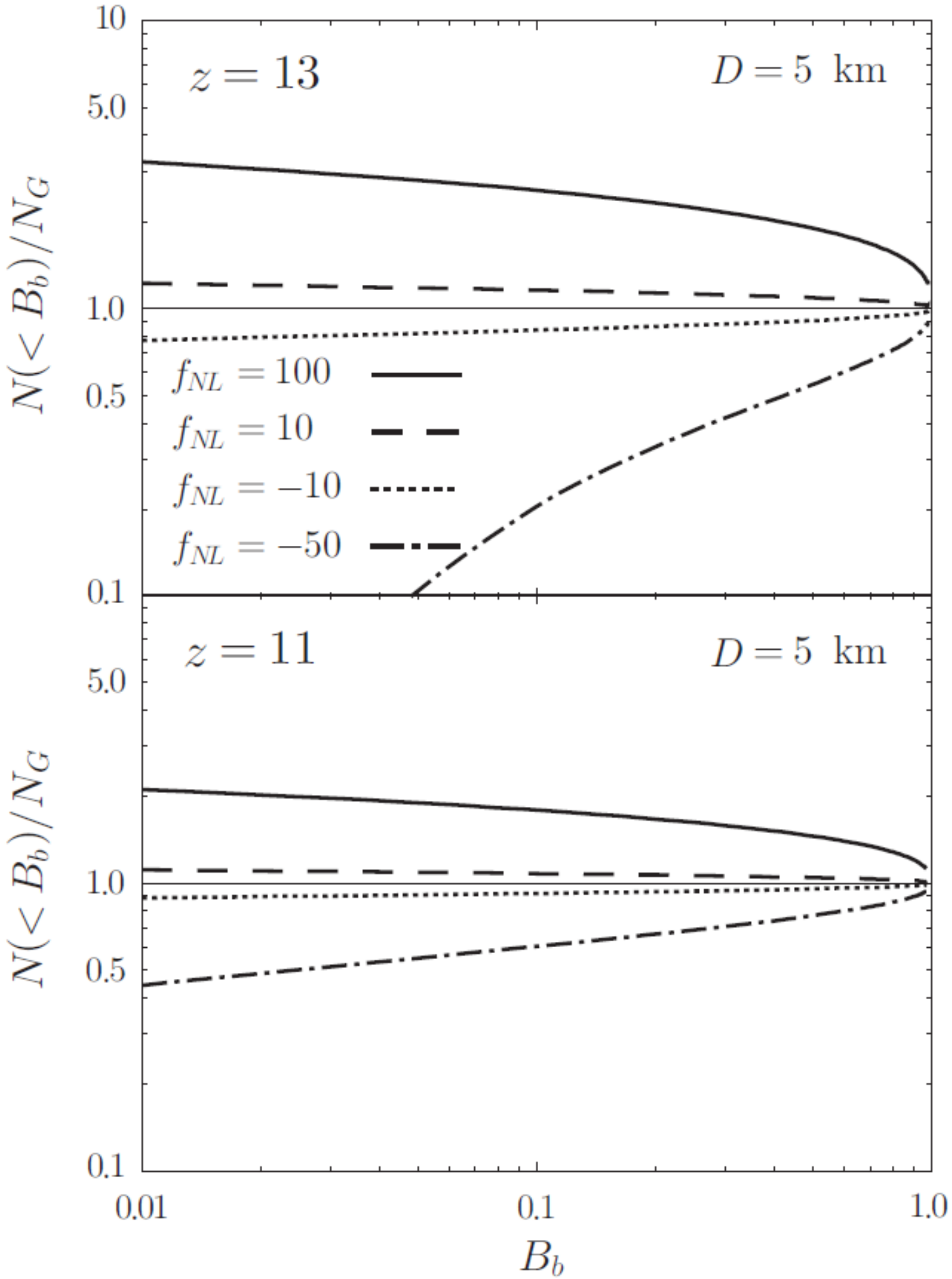

Ratio to the Gaussian case

(1) Smaller bubbles (larger B_b)

More numbers (not rare objects)

Less significant Non-Gaussianity

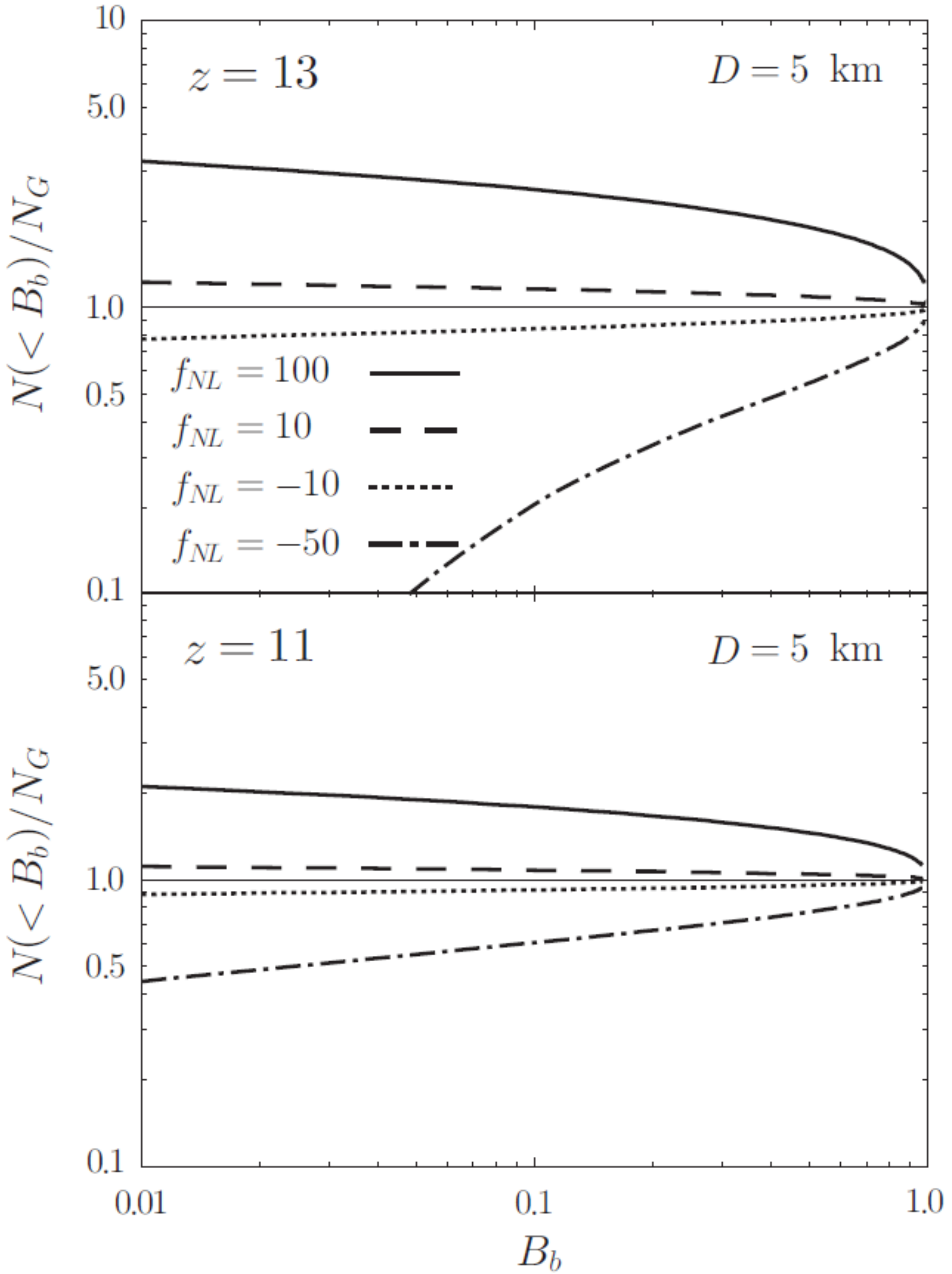

Ratio to the Gaussian case

(2) Higher redshift

Only rare objects can be collapsed

More significant Non-Gaussianity

Time evolution of deviation from the Gaussian case

Small bubbles

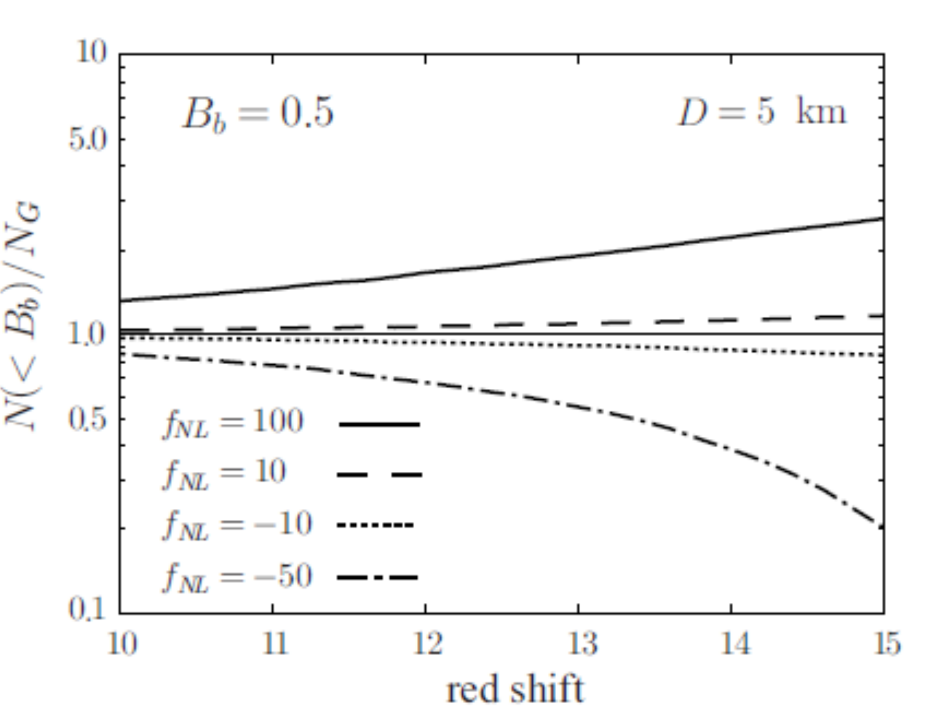

Large bubbles

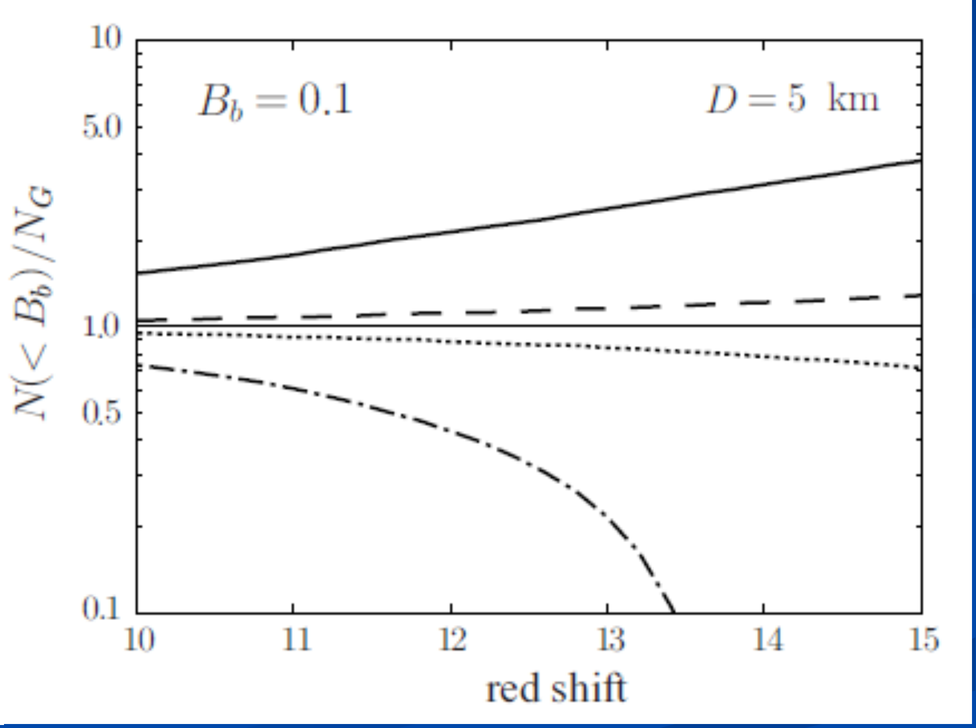

S/N: signal to noise ratio

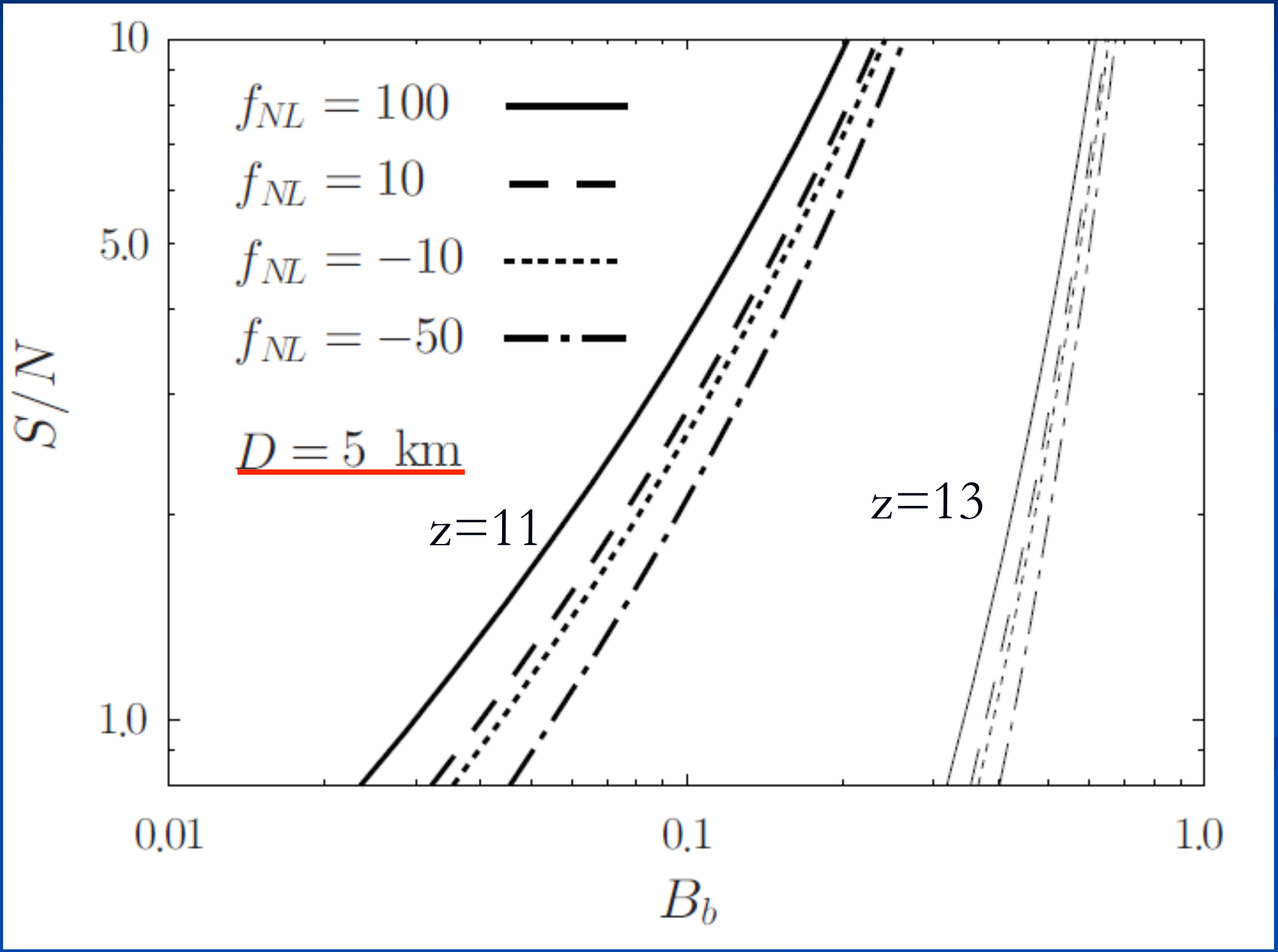

Summary

\# of Bubbles can be a good measure of Non-Gaussianity

- B_b
  - Smaller $B_b \rightarrow$ larger deviation from Gaussian
  - Smaller $B_b \rightarrow$ less number of Bubbles
  - Optimal B_b for given S/N
    - S/N=10, B_b =0.2 at z=11 ($N_{NG}(f_{NL}=100)/N_G \sim 1.7$)
    - S/N=3, B_b =0.1 at z=11 ($N_{NG}(f_{NL}=100)/N_G \sim 1.9$)
- z
  - Higher z $\rightarrow$ larger deviation from Gaussian
  - Higher z $\rightarrow$ Less number of bubbles
    - Ex) B_b=0.1, z=13 $\rightarrow$ $N_{NG}(f_{NL}=100)/N_G \sim 2.5$,
      BUT: $N_{NG}(f_{NL}=100)<1$